Pressure effects on the magnetic and transport properties of $Pr_{1-x}Sr_xMnO_3$ crystals near the percolation threshold

V. Markovich,[1,*] I. Fita,[2,3] R. Puzniak,[2] A. Wisniewski,[2] K. Suzuki,[4] J. W. Cochrane,[5] Y. Yuzhelevskii,[1] Ya. M. Mukovskii,[6] and G. Gorodetsky[1]

[1]*Department of Physics, Ben-Gurion University of the Negev, P.O. Box 653, 84105 Beer-Sheva, Israel*
[2]*Institute of Physics, Polish Academy of Sciences, Al. Lotnikow 32/46, PL 02-668 Warsaw, Poland*
[3]*Donetsk Institute for Physics & Technology, N A S, R. Luxemburg str. 72, 83114 Donetsk, Ukraine*
[4]*School of Physics & Materials Engineering, Monash University, P.O. Box 69M Clayton, Victoria 3800, Australia*
[5]*School of Physics, The University of New South Wales, Sydney 2052, Australia*
[6]*Moscow State Institute of Steel and Alloys, 119991 Moscow, Russia*

Effects of hydrostatic pressure up to 11 kbar on the magnetic and transport properties of $Pr_{1-x}Sr_xMnO_3$ (PSMO) were investigated in single crystals with various doping level: $x=0.22, 0.24, 0.26$, in a wide range of temperature. In similarity with other low doped manganites, PSMO exhibits a metal to insulator transition and magnetoresistance maxima at the same temperature $T=T_{MI}$. It was found that the magnetic ordering temperature T_C of the Mn spin sublattice and T_{MI} increase linearly upon applying the pressure. The pressure coefficients dT_C/dP and dT_{MI}/dP of PSMO enhance around percolation threshold at $x=x_C=0.24$ upon increasing the doping level. According to the magnetization measurements it appears that the nature of the ferro-to-paramagnetic phase transition in PSMO also varies at the crossover region, in a similar manner to that of $La_{1-x}Ca_xMnO_3$. At ambient pressure the transition for $x=0.22$ is of a second order while for $x=0.26$ it is of a first order, a nature of a transition for $x=0.24$ is not well defined yet. The effect of pressure of ~ 11 kbar on the kind of the magnetic phase transition is clearly seen in the case of $x=0.24$ sample. Applied pressure changes the character of the phase transition from nearly a continuous one at $P=0$ to more abrupt, almost discontinuous one at $P=10.7$ kbar. Measurements of magnetization and of ac susceptibility employed in our studies indicate upon an ordering of the Pr magnetic subsystem and a cluster glass behavior at temperatures $T_C(Pr)$ (80–100 K), much lower than T_C (165–205 K). All of the results obtained are discussed with regards to existing models of magnetic and transport properties of low doped manganites.

I. INTRODUCTION

Manganites of the form $(R_{1-x}A_x)MnO_3$ (R is a rare-earth ion and A is a divalent ion such as Ca, Sr, Ba, etc.) exhibit a plethora of magnetic and electronic phases, depending on the level of the doping x and the average A-site cation radius, $\langle r_A \rangle$.[1–3] The above-mentioned properties are related also to the tolerance factor tol$=(R_{1-x}A_x$—$O)/\sqrt{2}(Mn$—$O)$, where $R_{1-x}A_x$—O, Mn—O are the average cation–oxygen interatomic distances, values of which are usually calculated from the ionic sizes.[1,4] It is widely accepted that colossal magnetoresistance (CMR) arises mainly due to the double exchange (DE) interaction mediated by hopping of spin-polarized e_g electrons, between Mn^{3+} and Mn^{4+}, thereby facilitating both the electrical conductance and the ferromagnetic (FM) coupling, in the ferromagnetic metallic phase. On the other hand, certain electron orbital configurations energetically favor superexchange (SE) interactions between localized electrons and may yield a formation of ferromagnetic insulating or antiferromagnetic (AF) phases.

Details of the magnetic phase diagrams carrier concentration-transition temperature of CMR manganites are usually obtained by magnetic, structural, and transport measurements performed under applied magnetic field. The hydrostatic pressure (P) is yet another parameter, which can be used to change the equilibrium phase state of manganites. It

is generally acceptable that the Curie temperature T_C depends on the bandwidth W, described by the following expression suggested for perovskites:[5] $W=\cos \omega/(d_{Mn-O})^{3.5}$, where ω is the tilt angle in the plane of the bond and d_{Mn-O} is the Mn—O bond length. Though it is believed that the bandwidth scenario may explain qualitatively the $T_C(P)$ variation, one cannot exclude the important role of the Jahn–Teller distortion and its dependence on lattice deformation. For various optimally doped manganites ($x=0.3$) a definite trend in the dependence of dT_C/dP on T_C was established.[6] Namely, the higher dT_C/dP value corresponds to the lower T_C. It is generally accepted that such a trend is valid also for low-doped manganites.[7,8]

As already stated the magnetic and electric properties of manganites are very sensitive to external pressure, especially in the vicinity of percolation threshold x_C, i.e., of the critical doping level at which a crossover from a localized-type conductance at $x < x_C$ to itinerant one at $x > x_C$ occurs.[9,10] The calculations of the pressure dependence of Curie temperature have shown that dT_C/dP descends with the increase of doping for $x > x_C$. This result was confirmed experimentally in $La_{1-x}Ca_xMnO_3$ (LCMO) and in $La_{1-x}Sr_xMnO_3$, where dT_C/dP increases with doping at $x < x_C$, reaches a maximum near x_C and then decreases monotonically.[10] Recent studies of dT_C/dP for $La_{1-x}Ca_xMnO_3$ ($x=0.18, 0.2, 0.22$) crystals[11,12] showed that the sensitivity of T_C to external

TABLE I. Structural parameters, tolerance factor (tol), average A-site atomic radius, Curie temperature (T_C), pressure coefficients of T_C (dT_C/dP) and of metal–insulator transition temperature (dT_{MI}/dP), and paramagnetic Curie temperature (Θ) for PSMO crystals.

Composition	a(Å)	b(Å)	c(Å)	V(Å)^3	Tolerance factor (tol)	Average A-site atomic radius (Å)	T_C (K)	dT_C/dP (K/kbar)	dT_{MI}/dP (K/kbar)	Θ (K)
$Pr_{0.78}Sr_{0.22}MnO_3$	5.4951	7.7388	5.4847	233.24	0.9533	1.323	168±1	1.07±0.1	0.6±0.1	177±3
$Pr_{0.76}Sr_{0.24}MnO_3$	5.4836	7.7388	5.4886	232.92	0.9555	1.326	177±1	1.6±0.1	1.74±0.1	191±3
$Pr_{0.74}Sr_{0.26}MnO_3$	5.4775	7.7355	5.4845	232.38	0.9576	1.329	203±1	2.2±0.15	1.95±0.1	207±3

pressure is very low at $x < x_C$ ($dT_C/dP \approx 0.3$ K/kbar), while dT_C/dP is much higher for $x > x_C$. Moreover, in the vicinity of x_C a change in the nature of para-to-ferromagnetic transition was observed. Namely, in LCMO system the phase transition at T_C changes from a continuous second order one for low doping to a first order magnetic transition for $x > x_C$.[3,13–16]

The $Pr_{1-x}Sr_xMnO_3$ (PSMO) mimics in many ways the behavior of the classic LCMO system. The two systems have the same sequence of magnetic phases upon doping, comparable percolation threshold ($x_C = 0.22$ for LCMO[9] and $x_C = 0.24$ for PSMO[17]) and practically equal T_C at optimal doping ($T_C \sim 250$ K for $x = 0.3$). It is worth noting that for both systems the percolation threshold lies in the range of the critical tolerance factor $tol_c \approx 0.96$,[3] where the transition from orthorhombic ($c/a < \sqrt{2}$) to pseudocubic phase ($c/a \approx \sqrt{2}$) occurs.

In this work we report on the measurements of magnetization, ac susceptibility, and transport properties of hole doped $Pr_{1-x}Sr_xMnO_3$ crystals, having the level of the doping near the percolation threshold. The nature of the magnetic phase transition, the pressure effect on the Curie temperature, as well as spin-glass behavior are discussed in conjunction with recent data received on LCMO system.

II. EXPERIMENT

Single crystals of $Pr_{1-x}Sr_xMnO_3$ ($x = 0.22, 0.24, 0.26$) were grown by a floating zone technique, using radiative heating.[18] The phase compositions of the samples at room temperature were examined by x-ray diffraction. The unit cell of these crystals is orthorhombic having a *Pnma* space group, see Table I. Though ionic radius of Sr is greater than that of Pr [for twelve-fold oxygen coordination[1,4] Pr^{3+}(1.29 Å) and Sr^{2+}(1.44 Å)], increasing doping results in the decrease of unit cell volume. This observation may be attributed to a progressive decrease of Jahn–Teller distortions with increasing doping and a transition to rhombohedral symmetry with $R\bar{3}c$ space group at high enough level of the doping ($x > 0.3$).[19] The calculated average A-site ionic radii as well as the tolerance factors for PSMO crystals are listed in Table I. The variation of lattice parameters with doping as well as magnetization and resistvity data for $Pr_{1-x}Sr_xMnO_3$ ($x = 0.22, 0.24, 0.26$) crystals agree well with results previously published for polycrystalline samples of similar

composition.[17,19,20] The values of the magnetic ordering temperature for Mn spins (see Figs. 1 and 2 and Table I) are completely consistent with the phase diagram of $Pr_{1-x}Sr_xMnO_3$ series, which was constructed after exhaustive investigation of homogeneous and oxygen stoichiometric samples.[17] Cylinder-shape samples having a diameter of 1 mm and height of 4 mm with $\langle 100 \rangle$ axis of rotation were used for measurements of magnetization under hydrostatic pressure. The measurements were performed in the temperature range 4.2–250 K and magnetic fields up to 16 kOe, applied perpendicular to the rotation axis of the samples, using PAR (model 4500) vibrating sample magnetometer. Details of the magnetic measurements under pressure are presented
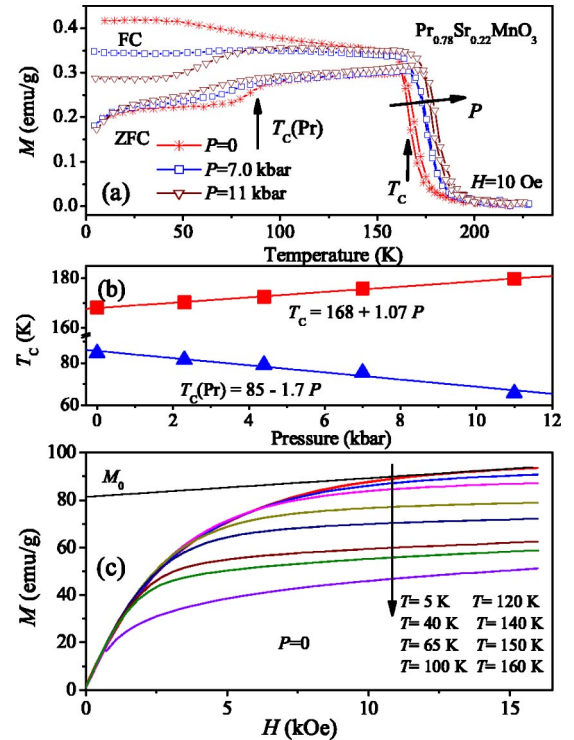
FIG. 1. (Color online) (a) Field cooled (M_{FC}) and zero field cooled magnetization (M_{ZFC}) of $Pr_{0.78}Sr_{0.22}MnO_3$ crystal, measured in an applied magnetic field $H = 10$ Oe for various pressures. (b) Pressure dependence of the magnetic ordering temperatures T_C and $T_C(Pr)$ of Mn and Pr ions, respectively. (c) Magnetic field dependencies of magnetization at various temperatures; M_0 is a spontaneous magnetization.

elsewhere.[11,12] A Lake Shore model-7310 ac-susceptometer was used for the measurements of magnetic susceptibility at a constant heating rate of about 2 K/min in temperature interval $20 \leqslant T \leqslant 300$ K. The ac magnetic field applied perpendicular to $\langle 100 \rangle$ direction was equal to 1.25 Oe. Samples for resistivity measurements were prepared in the form of parallepiped with dimensions of $5 \times 2 \times 1.6$ mm^3 and the longest dimension along the axis of as grown cylindrical crystal. Evaporated gold strips with a separation of about 0.5 mm between the voltage (V) contacts were used for the customary four-point resistance measurements. Measurements of magnetoresistance (MR) were carried out in a longitudinal geometry for which magnetic field H up to 15 kOe was aligned parallel to the current direction.

III. RESULTS

A. Magnetization

Figure 1(a) presents field cooled (FC) and zero field cooled (ZFC) magnetization curves, (M_{FC} and M_{ZFC}, respectively) of $Pr_{0.78}Sr_{0.22}MnO_3$ crystal, for H aligned along the easy axis in the (100) plane. The abrupt change in the magnetization at about $T \approx 165$ K is attributed to the magnetic ordering of the Mn sublattice. A change in the slope of M_{FC} and M_{ZFC} observed at $T \sim 80$ K occurs supposedly due to the ordering of Pr moments. Such ordering of Pr moments was found to be a characteristic feature of low doped $Pr_{1-x}Ca_xMnO_3$ (Ref. 21 and 22) and PSMO[20,23] systems. The Curie temperature of the Mn spin sublattice, T_C, at various pressures was determined by the inflection point of the magnetization curves. Observed difference between FC and ZFC curves is typical for canted spin antiferromagnets and spin glasses. In this work we have studied also the pressure dependence of the magnetic ordering temperature of Pr spin sublattice, $T_C(Pr)$ assigned by the maximal value of dM_{ZFC}/dT. The pressure dependencies of both ordering temperatures, T_C and $T_C(Pr)$ for $Pr_{0.78}Sr_{0.22}MnO_3$, are shown in Fig. 1(b). Observed pressure coefficients for both temperatures are remarkably different: $dT_C/dP \approx 1.07$ K/kbar while $dT_C(Pr)/dP \approx -1.7$ K/kbar; see Fig. 1(b). It should be noted that at higher pressures the change in the slopes of the magnetization curves at $T_C(Pr)$ is less pronounced and this hampers the determination of $T_C(Pr)$ and $dT_C(Pr)/dP$.

Magnetization curves $M(H)$ at various temperatures and under various pressures were measured also along the easy axis in the (100) plane. The $M(H)$ data have been used for determination of reduced magnetization, the temperature dependence of which is presented in the discussion. For ambient pressure $M(H)$ curves are presented in Fig. 1(c). A relatively high magnetic field of about 10 kOe is required to saturate the magnetization at $T=5$ K. At this temperature and for $H=16$ kOe, the magnetization reaches a value of 3.88 μ_B/f.u. at ambient pressure and 3.94 μ_B/f.u. at $P =11$ kbar.

Figure 2(a) shows FC and ZFC magnetization curves of $Pr_{0.76}Sr_{0.24}MnO_3$ crystal also for H aligned along the easy direction in the (100) plane. The following features are noticeable: (i) a kink in the $M_{FC}(T)$ curve appears near T_C at
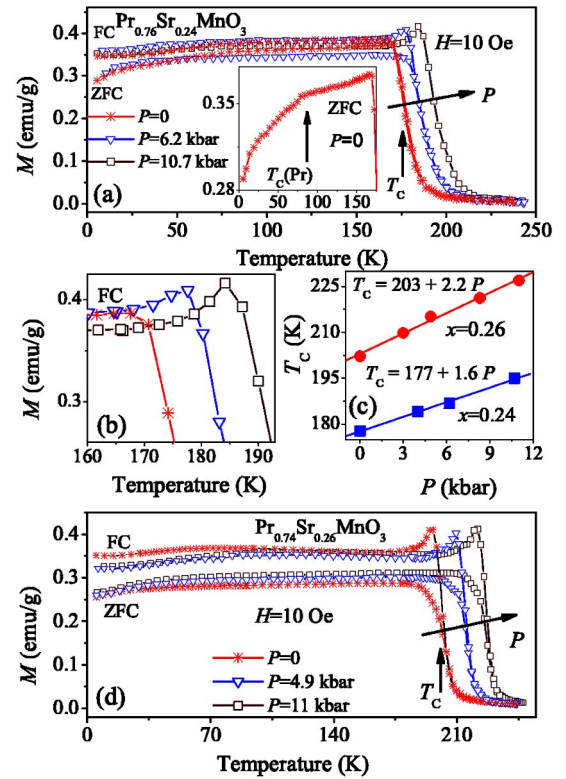
FIG. 2. (Color online) (a) Field cooled M_{FC} and zero field cooled magnetization M_{ZFC} of $Pr_{0.76}Sr_{0.24}MnO_3$ crystal, measured in an applied magnetic field $H=10$ Oe for various pressures. The change in the slope of ZFC curve at ambient pressure is enlarged in the inset. (b) The evolution of the kink in $M_{FC}(T)$ for $x=0.24$ with pressure. (c) Pressure dependence of T_C for $x=0.24$ and for $x =0.26$ crystals. (d) Field cooled M_{FC} and zero field cooled magnetization M_{ZFC} of $Pr_{0.74}Sr_{0.26}MnO_3$ crystal, measured in an applied magnetic field $H=10$ Oe for various pressures.

$P \sim 4$ kbar—this kink increases with increasing pressure [Fig. 2(b)]; (ii) the temperature T_C increases with increasing pressure from 177 K at $P=0$ up to 195 K for $P=10.7$ kbar, thus exhibiting a pressure coefficient $dT_C/dP \approx 1.6$ K/kbar [Fig. 2(c)]; (iii) the change in the slope of M_{FC} and M_{ZFC} curves (at $T \approx 80$ K for $P=0$) is attributed to the ordering of Pr moments [see the inset to Fig. 2(a)]. Under applied pressure this change in the slope of both magnetization curves at $T_C(Pr)$ is faintly discernible. At $T=5$ K and $H=16$ kOe the magnetization reaches a value of 3.91 μ_B/f.u. and this quantity remains practically unchanged under an applied pressure. Finally, Fig. 2(d) presents FC and ZFC magnetization curves, of $Pr_{0.74}Sr_{0.26}MnO_3$ crystal, for H aligned along the easy direction in the (100) plane. The abrupt change in the magnetization at about $T \approx 200$ K occurs due to the magnetic ordering of the Mn spins (T_C). The following features were observed: (i) the temperature T_C increases linearly with pressure from 203 K at $P=0$ up to 227 K for $P=11$ kbar, hence exhibiting a pressure coefficient $dT_C/dP \approx 2.2$ K/kbar [Fig. 2(c)]; (ii) the kink in the $M_{FC}(T)$ curve around T_C is visible at all pressures and it is more pronounced than that of the $x =0.24$ sample; (iii) a very slight change in the slope at low temperatures ~ 60 K is visible only for the M_{FC} curves. At
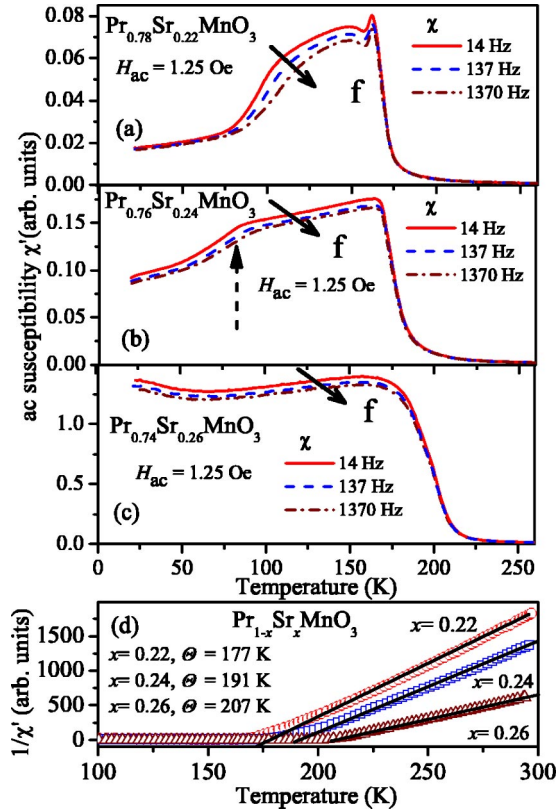
FIG. 3. (Color online) (a) Temperature dependence of the ac susceptibility χ' measured at different frequencies for (a) $Pr_{0.78}Sr_{0.22}MnO_3$ single crystal; (b) $Pr_{0.76}Sr_{0.24}MnO_3$ single crystal. Dashed arrow shows the position of bending point of χ'; (c) $Pr_{0.74}Sr_{0.26}MnO_3$ single crystal; (d) Temperature dependence of the inverse magnetic susceptibility of $Pr_{1-x}Sr_xMnO_3$ single crystals. The susceptibility obeys Curie–Weiss law in the high-temperature region.

$T = 5$ K and $H = 16$ kOe the magnetization reaches a value of 3.87 μ_B/f.u. at $P = 0$ and again this quantity remains almost unchanged under an applied pressure.

B. ac magnetic susceptibility

The results obtained for the ac susceptibility versus temperature, at different frequencies are presented in Fig. 3. We show the real part, χ' only, because experimental problem in the determination of χ'' arises due to the small phase shift with increasing temperature. Since the imaginary part χ'' is much smaller than χ', real part χ' coincides practically with total susceptibility χ. A sharp peak in χ' was observed for PSMO crystals at ferromagnetic transition temperature of the Mn spin sublattice, plausibly associated with the critical softening of the ferromagnetic system near T_C, see Figs. 3(a)–3(c). In addition to that a sharp drop in χ' was observed around 100 K for $x = 0.22$ sample, see Fig. 3(a). The above-mentioned effects were found to exhibit distinct frequency dependence. With increasing doping the anomalies of ac susceptibility become less pronounced [$x = 0.24$ case, see Fig. 3(b)] and practically disappear for $x = 0.26$ [see Fig. 3(c)]. This behavior resembles that one previously observed in low
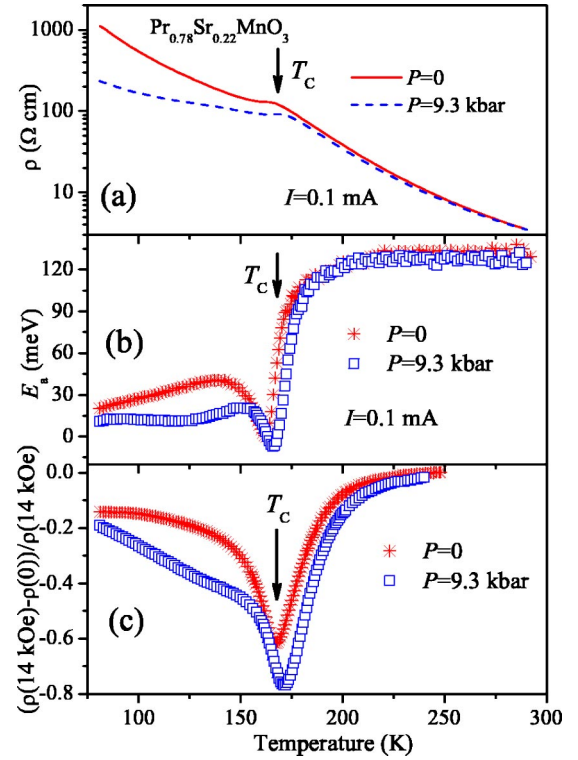
FIG. 4. (Color online) (a) The resistivity of the $Pr_{0.78}Sr_{0.22}MnO_3$ crystal as a function of temperature at ambient pressure and at $P = 9.3$ kbar. (b) Temperature dependence of the activation energy determined numerically by calculating $d\ln(\rho)/d(k_BT)^{-1}$ from resistivity data for $P = 0$ and $P = 9.3$ kbar. (c) Temperature dependence of magnetoresistance for $P = 0$ and $P = 9.3$ kbar.

doped ($x = 0.18, 0.2, 0.22$) LCMO crystals.[11,12] The inverse susceptibility χ^{-1} vs temperature [Fig. 3(d)] obeys Curie–Weiss law $\chi^{-1} = (T - \Theta)/C$. The values of Θ obtained are listed in Table I. As expected, Θ increases with increasing doping.

C. Resistance and magnetoresistance

Similar to LCMO crystals,[24] all PSMO single crystals were twinned with small mosaicity, and therefore anisotropy effects visible in magnetization measurements were almost fully hidden in transport measurements. Figure 4(a) presents the temperature dependence of the resistivity $\rho(T)$ for $x = 0.22$ sample at $P = 0$ and $P = 9.3$ kbar determined at electric current of $I = 100$ μA upon slow heating. At $T < T_C$, the resistivity of this sample becomes strongly current dependent.[25] Similar to the behavior of low doped LCMO crystals with $x = 0.18$ and 0.2,[24] an application of high enough current at low temperatures produces transitions to a metastable state with lower resistivity.[25] Let us underline that the resistivity measured in the heating and cooling runs, practically coincides, hence only data gathered during heating are shown in Fig. 4(a). At temperatures well above T_C, the resistivity can be well fitted by Arrhenius law of the form $\rho(T) = \rho_0 \exp(E_a/k_BT)$. The activation energy E_a of the $Pr_{0.78}Sr_{0.22}MnO_3$ sample at temperatures 210–300 K is about 125–130 meV and is much lower at lower temperatures, see
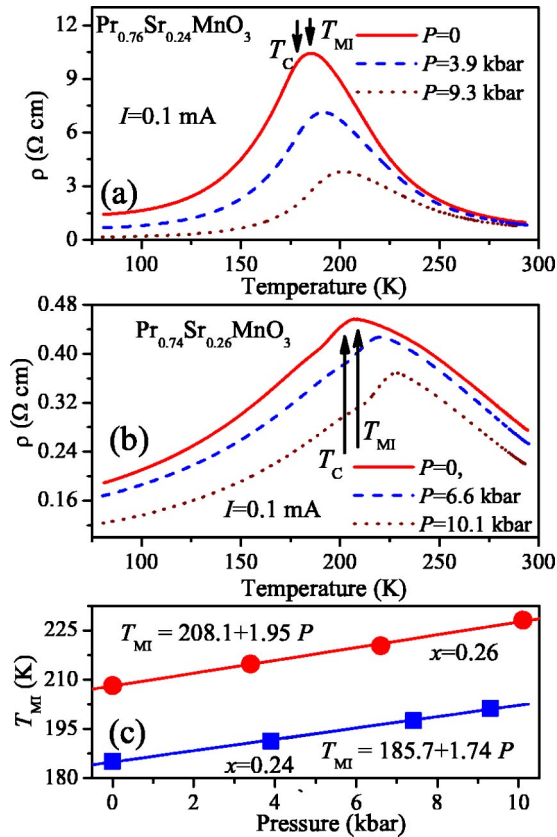
FIG. 5. (Color online) The resistivity of the $Pr_{0.76}Sr_{0.24}MnO_3$ (a) and of $Pr_{0.74}Sr_{0.26}MnO_3$ (b) crystals as a function of temperature at various pressures. (c) The pressure dependence of MI transition temperature for $x=0.24$ and for $x=0.26$ crystals.

Fig. 4(b). The change in the activation energy E_a points out possible changes in the conduction mechanism, i.e., the marked drop in the activation energy, seen at T_C [Fig. 4(b)] are characteristic feature of magnetic semiconductors, where E_a depends strongly on the long-range magnetic order and the alignment of atomic magnetic moments reinforces the probability of electron transfer between Mn sites.[26] It was found that an applied pressure reduces strongly the resistivity below T_C, while such effect is very small at temperatures $T > T_C$. The effect of pressure on the magnetoresistance of $Pr_{0.78}Sr_{0.22}MnO_3$ crystal is shown in Fig. 4(c). At $P=0$ and in the vicinity of T_C the MR is approaching almost 60%, under pressure of $P=9.3$ kbar the MR is about 80%, resembling the results for low doped LCMO manganites.[12] The temperature shift of the bending point in $\rho(T)$ [Fig. 4(a)] as well as temperature shifts of the minimums of $E_a(T)$ [Fig. 4(b)] and of $MR(T)$ [Fig. 4(c)] are of about $\Delta T=5–5.5$ K under a pressure of 9.3 kbar. This enables us to estimate the pressure coefficient at the temperature where the conductance mechanism changes, i.e., $dT_{MI}/dP \approx 0.6$ K/kbar, in spite of the fact that metal–insulator (MI) transition is hardly seen in the resistivity of $Pr_{0.78}Sr_{0.22}MnO_3$ crystal [Fig. 4(a)].

Figure 5(a) shows the temperature dependence of the resistivity $\rho(T)$ for $x=0.24$ at electric current $I=100$ μA, upon slow heating at various pressures. The ferromagnetic transition temperature of the Mn spin sublattice T_C (Fig. 2) is

somewhat lower than the MI transition temperature, determined by the resistivity peak; see Fig. 5(a). The shift of the MI transition under pressure [see Fig. 5(c)] is similar to that of T_C [Fig. 2(c)]. At temperatures below T_C, the resistivity exhibits quasimetallic behavior ($d\rho/dT > 0$). Moreover, it demonstrates nonlinear conduction below T_C, albeit in less pronounced manner than that for the $x=0.22$ crystal.[25] The resistivity can be fitted by a simple Arrhenius expression only at high temperatures, above 220 K with $E_a \approx 150$ meV. It can also be reliably concluded that E_a decreases slightly under pressure. At $P=0$ and in the vicinity of T_C the MR is approaching almost $\sim 75\%$ and at $P=9.3$ kbar the MR increases up to $\sim 95\%$. Temperature dependence of the resistivity $\rho(T)$ of $Pr_{0.74}Sr_{0.26}MnO_3$ crystal at various pressures is shown in Fig. 5(b). Here again, T_C [Figs. 2(c) and 2(d)] is somewhat lower than the MI transition temperature. The shift of the MI transition temperature under pressure [see Fig. 5(c)] is compatible with the corresponding shift of T_C [see Fig. 2(c)]. In distinct contrast with the behavior of $Pr_{0.78}Sr_{0.22}MnO_3$ crystal, the resistivity of $x=0.24$ and 0.26 samples is metallic below T_C. At $P=0$ and in the vicinity of T_C the MR is about 11% only. An applied pressure causes a small increase of MR and near T_C at $P=10.1$ kbar the MR approaches about 20%.

IV. DISCUSSION

The magnetization of PSMO crystals measured at $T=5$ K along the easy axis in the (100) plane and in a magnetic field of $H=16$ kOe approaches values higher than that expected for the magnetic moment of Mn spins of Mn^{3+} and Mn^{4+}. For the present ratios of Mn^{3+} and Mn^{4+} one expects to get 3.78 $\mu_B/f.u.$, 3.76 $\mu_B/f.u.$, 3.74 $\mu_B/f.u.$, for PSMO crystals with $x=0.22, 0.24, 0.26$, respectively. Moreover, the distinctive anomalies in $M(T)$ indicate upon a spin ordering of Pr ions. It should be noted that in some Pr-based manganites [$Pr_{0.74}Sr_{0.26}MnO_3$ (Ref. 20) and $Pr_{0.8}Ca_{0.2}MnO_3$ (Ref. 23)] the magnetic ordering of Pr^{3+} ions manifests itself only in slight change in the slope of $M(T)$ due to predominant contribution of Mn spins. The superexchange interaction between Pr ions and neighboring Mn ions depends on the charge, crystallographic structures, and the relative orientation of the corresponding orbitals.[21]

Though the pressure effect on T_C and FM interactions was extensively studied in the past for various perovskite manganites (Refs. 1, 3, 5–9, 11, and 12, and references therein), there is a diversity in the values of the pressure coefficients of the Curie temperature reported for the vicinity of the x_C. This is mostly connected with the fact that early studies of manganites were plagued by a variable oxygen stoichiometry, particularly for the compositions with smaller x.[3] Another source of error may occur when a pressure coefficient dT_C/dP is evaluated from the resistivity measurements. Cui and Tyson have shown recently that for many manganites the magnetic and electronic transitions may be significantly decoupled, especially under high pressures.[27] The decoupling of T_C and T_{MI} is ascribed to the competition between DE and SE interactions of neighboring Mn—Mn spins. This scenario is enforced in the vicinity of the percolation threshold,
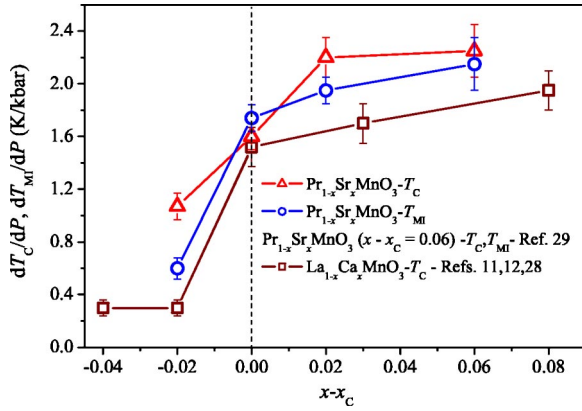
FIG. 6. (Color online) The pressure coefficients of ferromagnetic T_C and metal-insulator T_{MI} transition temperatures of $Pr_{1-x}Sr_xMnO_3$ single crystals as a function of doping; x_C denotes doping at which a crossover from a localized type conductance ($x < x_C$) to itinerant one ($x > x_C$) occurs.

where the above competition manifests itself also in a competition between hopping conductivity in the paramagnetic phase and metallic-percolative conductivity, resulting in a resistivity maximum at T_{MI}.[1,2] An applied pressure may change the percolative state, affecting the different conduction channels and in turn results in a variation of T_C and T_{MI}. Figure 6 presents the pressure coefficient of the Curie temperature and MI transition temperature of PSMO crystals (Figs. 1, 2, 4, and 5). For comparison, the pressure coefficients for LCMO crystals[11,12,28] and $Pr_{0.7}Sr_{0.3}MnO_3$ (Ref. 29) are also shown in Fig. 6. The above-noted results indicate that the pressure coefficient dT_C/dP exhibits a sharp change in the vicinity of x_C and varies only slightly with increasing doping up to $x \sim 0.3$. In recent investigations of $La_{0.75}Ca_{0.25}MnO_3$ by infrared absorption[30] the value of dT_{MI}/dP was found to be 2.3 K/kbar, in compliance with our observation. The enhanced change in dT_C/dP at x_C was attributed to the different nature of magnetic interactions below and above x_C.[11,12] In the case of $x > x_C$, DE dominates the magnetic and transport properties, whereas at $x < x_C$ DE is partly replaced by another type of FM interaction, e.g., superexchange. Double exchange is more sensitive to pressure than SE, and therefore the pressure coefficients dT_C/dP and dT_{MI}/dP enhance above x_C. It is generally believed (at least in modest pressure regime $P < 20$ kbar) that an external pressure acts similarly to chemical doping with larger atoms.[1,30] Both tend to increase the Mn—O—Mn bond angle and to compress Mn—O—Mn bond length, thereby leading to larger e_g bandwidth, and consequently to higher values of T_C and of T_{MI}. In order to compare Mn—O bond lengths and the Mn—O—Mn bond angles in both systems under consideration (PSMO and LCMO) we have recalculated existing room temperature neutron data for $La_{0.75}Ca_{0.25}MnO_3$ (Ref. 31) and $Pr_{0.7}Sr_{0.3}MnO_3$ (Ref. 19) with a *Pnma* orthorhombic cell. The following values were obtained for $La_{0.75}Ca_{0.25}MnO_3$: planar bond lengths Mn—O2 are 1.9646 and 1.9732 Å, apical bond length Mn—O1 is 1.9709 Å, planar Mn—O2—Mn angle is 160.8°, and apical Mn—O1—Mn angle is 159.07°. The small difference in planar bond lengths signals on a presence

of $Q2$ orthorhombic distortion with the in-plane bonds differentiating in a long and a short one. The structural parameters observed for $Pr_{0.7}Sr_{0.3}MnO_3$ are: planar bond lengths Mn—O2 are 1.9622 and 1.9653 Å, apical bond length Mn—O1 is 1.9597 Å, planar Mn—O2—Mn angle is 160.9°, and apical Mn—O1—Mn angle is 160.7°. Both compounds have rather small orthorhombic distortions with similar values of Mn—O—Mn bond angles and Mn—O bond lengths and this fact allows us to discuss the pressure effect on T_C in both systems from a common point of view. The pressure effect on T_C is larger than that predicted by band theory. This occurs because of the reduction of electron–phonon (el–ph) coupling under applied pressure,[30] which leads to the enhancement of the electron mobility.

Recently, Postorino *et al.*[32] calculated the pressure dependence of T_C based on a model of two-site Mn cluster. Their model includes several competing couplings like: DE, Hund, AF–SE coupling, and el–ph interactions. The authors have shown that the pressure dependence of Hund's coupling can be safely assumed to be identical for $x = 0.25$ and $x = 0.33$. Using the results obtained by Sacchetti *et al.*[33] one may express the hopping integral under pressure by an empirical expression $t(P) = t(0)[1 + 0.001P$ (kbar)]. Taking into account the proportionality between t and T_C at $P = 0$ (Ref. 1) (valid for $x > x_C$) one may conclude that the increase in the hopping integral alone cannot account quantitatively for the values of dT_C/dP obtained for LCMO and PSMO and the effect of pressure on the el–ph coupling should be taken into account. The pressure dependence of el–ph coupling for LCMO with $x = 0.25$ was calculated[33] by using the pressure dependence of Jahn–Teller phonon frequency. The results show that a remarkable pressure induced reduction of el–ph coupling ($\sim 7\%$ at 10 kbar) is observed even at modest pressures. This behavior is found to be consistent with the enhancement of the metallic character of resistivity and an increase of T_C under pressure for both LCMO and PSMO systems at $x_C < x < \sim 0.3$ (see Refs. 29–33 and Figs. 1, 2, 4, and 5).

One of the open issues of hole-doped manganites is the nature of magnetic transition at T_C. In the case of, e.g., LCMO system (see Refs. 14–17 and 34) it was shown that the nature of the para-to-ferromagnetic transition (PFT) at T_C depends on the level of Ca-doping. Such a transition was found to be of a first order for $x \sim 0.3$,[14–16] while for $x = 0.2$ and $x > 0.4$[16,34] it is of a second order and for $x = 0.27$ PFT exhibits a combination of characteristics associated with both first-order and second-order transitions simultaneously.[16] Rivadulla *et al.*[34] have shown recently that the PFT of LCMO is of a first order only in compositional range $0.275 < x < 0.43$, whereas close to the localized-to-itinerant electronic transition, at $x \approx 0.2$ and $x \approx 0.5$ the system does not undergo a true magnetic transition due to an occurrence of a random field which breaks up the electronic/magnetic homogeneity of the system. Our analysis of the nature of PFT in PSMO will be based on the classical model of Bean and Rodbell (BR),[35] for which a linear approximation of the Curie temperature dependence on the lattice deformation is assumed, i.e.,

$$T_C = T_{C0}[1 + \beta(V - V_0)/V_0], \tag{1}$$

where T_{C0} denotes the Curie temperature of an uncompressible lattice of volume V, i.e., at zero pressure, V_0 is the vol-
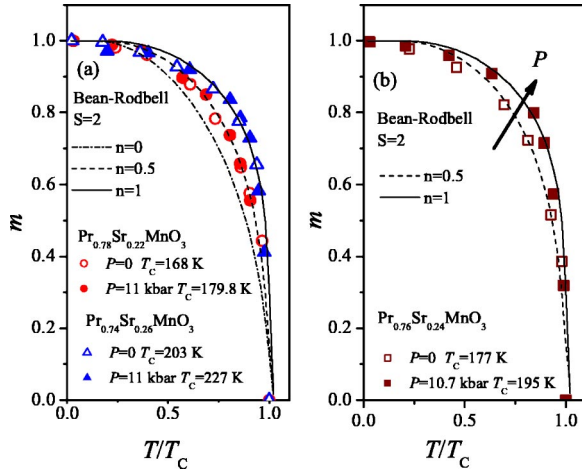
FIG. 7. (Color online) The temperature dependence of the reduced magnetization m at $P=0$ and under applied pressure: (a) for $Pr_{1-x}Sr_xMnO_3$ ($x=0.22, 0.26$) single crystals; (b) for $Pr_{1-x}Sr_xMnO_3$ ($x=0.24$) single crystal. The experimental results are compared with prediction of the model of Bean–Rodbell.

ume in the absence of exchange interactions and magnetic ordering, and β is the slope of T_C vs V dependence. Using the molecular field approximation Bean and Rodbell[35] have found that

$$T/T_C = (m/\tanh^{-1} m)(1 + nm^2/3 - PK\beta), \qquad (2)$$

where coupling parameter $n=(3/2)Nk_BKT_{C0}\beta^2$, N is the number of interacting atoms per unit volume, m is reduced magnetization, and K is isothermal compressibility given by $K=-V^{-1}(\partial V/\partial P)$. For $n<1$, the magnetic transition is of a second order, whereas for $n>1$ it is of a first-order transition.

Figure 7 shows the temperature dependence of the reduced magnetization m of PSMO crystals determined from magnetization measurements under ambient and applied pressure as well as calculated curves within BR model for spin $S=2$ and for pressure value set to zero. It is clearly seen [Fig. 7(a)] that character of reduced magnetization for $x=0.22$ sample is quite different from that of $x=0.26$ sample, and their characteristic features do not depend on the applied pressure. One may consider the PFT of $x=0.22$ sample as a second order ($n\sim0.5$), whereas for $x=0.26$ the PFT is almost discontinuous ($n\sim1$). Figure 7(b) shows that the character of PFT for $x=0.24$ changes under pressure from nearly a continuous one ($n\sim0.5$) to almost discontinuous transition ($n\sim1$). A kink in M_{FC} near PFT [Figs. 2(a) and 2(d)] for $x=0.24, 0.26$ and the corresponding difference between M_{FC} and M_{ZFC} may be an indicative sign of first order of PFT and possibly of a spontaneous magnetostriction,[14] in some resemblance with the results reported recently[36] for $(La_{0.7}Ca_{0.3})_{1-x}Mn_{1+x}O_3$ manganites.

Novak et al.[14] applied the BR model for the analysis of the nature of PFT in manganites governed by DE interactions. They received results similar to those obtained within original BR model with respect to the nature of PFT. More-

over, they have shown that the coupling parameter n and dT_C/dP can be related by[14]

$$n = \frac{35S(S+1)}{6(S-1)(3S+1)} \frac{Nk_B}{kT_C} \left(\frac{dT_C}{dP}\right)^2, \qquad (3)$$

where

$$k = -\frac{1}{(d_{Mn-O})} \frac{\partial(d_{Mn-O})}{\partial P}$$

is the compressibility of Mn—O bond. Radaelli et al.[31] have found that variation of Mn—O length with external pressure in optimally doped manganites is approximately the same for several manganites $(R_{1-x}A_x)MnO_3$, where $R=La, Pr$; $A=Ca, Sr, Ba$;, $k=2.32\times10^{-4}$ kbar^{-1}. Using this value and the values of dT_C/dP given in Table I, we have obtained the following values for n: 0.34, 0.80, and 1.21 for $x=0.22$, 0.24 and 0.26, respectively. These results are found to be in fair agreement with the experimentally observed PFT and resemble closely those found for LCMO system[13–16,34] at the percolative crossover.

Existing experimental data demonstrate that the phase separated state of manganites shares some similarities with classical spin-glass systems.[2,37] We have found recently that in low doped LCMO the spin-glass-like behavior manifests itself by a number of specific magnetic features,[11,12,24] e.g., the characteristic splitting between M_{FC} and M_{ZFC} below T_C and a frequency dependence of magnetic susceptibility. Among the PSMO crystals the most pronounced effect was observed for the $x=0.22$ sample. The onset of the decrease of χ' moves, as expected for spin glass, toward higher temperatures with increasing frequencies. This frequency shift attributed to relaxation phenomena in the spin glass system is characterized by a factor of the form:[37]

$$\eta = \frac{\Delta T_{cusp}}{T_{cusp}\Delta(\log \omega)}, \qquad (4)$$

where ΔT_{cusp} refers to temperature shift of the maximum of $d\chi'/dT$ at a given frequency difference. These values of η observed for $x=0.22$ and 0.24 samples lie in the region 0.04–0.06, typical for spin glasses[37] and are very similar to that observed previously in low doped LCMO with $x=0.2$.[24]

For the examination of the frequency shift of the glass freezing temperature we may apply the Arrhenius law of the following form:

$$f = f_0 \exp(-E_{ac}/k_BT_f). \qquad (5)$$

Here, f is the driving frequency of our ac susceptibility measurements, T_f is the freezing temperature, E_{ac} is the activation energy, and f_0 is the frequency of attempts for a cluster to change its spin direction. By plotting $\ln f$ vs. $1/T_f$ one determines: $E_{ac}=0.37\pm0.03$ eV and $E_{ac}=0.40\pm0.03$ eV, for $x=0.22$ and $x=0.24$, respectively. The obtained values coincide pretty well with values obtained for low doped LCMO ($x=0.18$ and $x=0.2$) crystals.[11,12]

In general the critical slowing down of spin glasses is characterized by a relaxation time τ, which diverges at the critical freezing point[37]

$$\tau_{\max} = \tau_0 \left(\frac{T_f - T_G}{T_G} \right)^{-z\nu}. \tag{6}$$

Here τ_0 is the shortest relaxation time available in the system, $z\nu$ is the dynamical exponent, T_G is the glass transition temperature, and T_f is the freezing temperature. By identifying $\tau_{\max}$ with the inverse of the measuring frequency and temperature of anomaly of the frequency dependent susceptibility curves with the freezing temperature T_f, we have obtained by the nonlinear fit with Eq. (6): $\tau_0 = 10^{-9}$ s, $z\nu = 12$, for the transition temperatures: $T_G = 80.2$ K ($x = 0.22$) and $T_G = 68.0$ K ($x = 0.24$). The values of the dynamical exponent are similar to those calculated previously for low doped LCMO crystals. Unexpectedly, τ_0 appears to be three orders of magnitude higher than that observed previously in LCMO ($\tau_0 \sim 10^{-12}$ s).[24,38] One must take into account that magnetic interactions in a nanoparticle cluster glass may yield similar characteristic values of $\tau_0 \sim 10^{-9}$ s.[38]

V. CONCLUSIONS

In summary, experiments involving measurements of magnetization and resistivity under pressure, and ac susceptibility at various frequencies were employed in our studies of magnetic states in low-doped $Pr_{1-x}Sr_xMnO_3$ ($x = 0.22, 0.24, 0.26$) single crystals. Our results show that similar to $La_{1-x}Ca_xMnO_3$, the nature of the ferro-to-paramagnetic transition of the Mn spin system changes with increasing doping from a continuous second-order transition to a more abrupt first-order-like transition. For $Pr_{0.76}Sr_{0.24}MnO_3$ an applied pressure results in more abrupt phase transition. It was found that the pressure coefficient of the Curie temperature for LCMO and PSMO systems is enhanced near the localized-to-itinerant electronic transition ($x_C = 0.22$ and 0.24 for LCMO and PSMO, respectively) and then it only slightly changes with increasing doping up to $x \sim 0.3$. It was found that the resistivity $\rho(T)$ of $x = 0.22$ crystal obeys Arrhenius law at $200 \text{ K} \leq T \leq 300 \text{ K}$ with an activation energy $E_a \approx 130$ meV, whereas below the T_C at $80 \text{ K} < T < 150 \text{ K}$, $E_a \approx 20$ meV. For temperatures in between, Arrhenius law does not hold presumably because of magnetic and electronic inhomogeneities.

Frequency-dependent glassy behavior was found for $x = 0.22$ and for 0.24 samples. The presence of the glassy transition has been also evidenced in the difference between ZFC and FC behavior and the frequency dependence of the freezing temperature, which can be reasonably well described by the conventional critical slowing-down law. The cluster glass temperature T_G decreases with increasing doping, analogous to that in LCMO case.[3,24,38]

---

*Email address: markoviv@bgumail.bgu.ac.il

[1] J. M. D. Coey, M. Viret, and S. von Molnar, Adv. Phys. **48**, 167 (1999).

[2] E. Dagotto, *Nanoscale Phase Separation and Colossal Magnetoresistance* Springer Series in Solid State Physics (Springer, Berlin, 2003).

[3] J. B. Goodenough, *Rare Earth-Manganese Perovskites* Handbook on the Physics and Chemistry of Rare Earth, Vol. 33 edited by K. A. Gschneidner Jr., J.-C. G. Bunzli, and V. Pecharsky (Elsevier Science, Amsterdam, 2003).

[4] R. D. Shannon, Acta Crystallogr., Sect. A: Cryst. Phys., Diffr., Theor. Gen. Crystallogr. **32**, 751 (1976).

[5] M. Medarde, J. Mesot, P. Lacorre, S. Rosenkranz, P. Fisher, and K. Gobrecht, Phys. Rev. B **52**, 9248 (1995).

[6] V. Laukhin, J. Fontcuberta, J. L. Garcia-Munoz, and X. Obradors, Phys. Rev. B **56**, R10 009 (1997).

[7] R. Shen and Z. Z. Li, Solid State Commun. **105**, 41 (1998).

[8] G.-M. Zhao, K. Conder, H. Keller, and K. A. Muller, Phys. Rev. B **60**, 11 914 (1999).

[9] T. Okuda, Y. Tomioka, A. Asamitsu, and Y. Tokura, Phys. Rev. B **61**, 8009 (2000).

[10] G.-M. Zhao, H. Keller, R. L. Green, and K. A. Muller, in *Physics of Manganites*, edited by T. A. Kaplan and S. D. Mahanti (Kluwer/Plenum, New York, 1999), pp. 221–241.

[11] V. Markovich, E. Rozenberg, A. I. Shames, G. Gorodetsky, I. Fita, K. Suzuki, R. Puzniak, D. A. Shulyatev, and Y. M. Mukovskii, Phys. Rev. B **65**, 144402 (2002).

[12] V. Markovich, I. Fita, R. Puzniak, M. I. Tsindlekht, A. Wisniewski, and G. Gorodetsky, Phys. Rev. B **66**, 094409 (2002).

[13] D. Kim, B. Revaz, B. L. Zink, F. Hellman, J. J. Rhyne, and J. F. Mitchell, Phys. Rev. Lett. **89**, 227202 (2002).

[14] P. Novak, M. Marysko, M. M. Savosta, and A. N. Ulyanov, Phys. Rev. B **60**, 6655 (1999).

[15] J. Mira, J. Rivas, F. Rivadulla, C. Vazquez-Vazquez, and M. A. Lopez-Quintela, Phys. Rev. B **60**, 2998 (1999); J. Mira, J. Rivas, L. F. Hueso, F. Rivadulla, M. A. Lopez-Quintela, M. A. Senaris Rodriguez, and C. A. Ramos, *ibid.* **65**, 024418 (2001).

[16] C. P. Adams, J. W. Lynn, V. N. Smolyaninova, A. Biswas, R. L. Greene, W. Ratcliff II, S. W. Cheong, Y. M. Mukovskii, and D. A. Shulyatev, Phys. Rev. B **70**, 134414 (2004); W. Li, H. P. Kunkel, X. Z. Zhou, Gwyn Williams, Y. Mukovskii, and D. Shulyatev, J. Phys.: Condens. Matter **16**, L109 (2004).

[17] C. Martin, A. Maignan, M. Hervieu, and B. Raveau, Phys. Rev. B **60**, 12191 (1999); M. Hervieu, G. Van Tendeloo, V. Caignaert, A. Maignan, and B. Raveau, *ibid.* **53**, 14 274 (1996).

[18] D. Shulyatev, S. Karabashev, A. Arsenov, and Ya. Mukovskii, J. Cryst. Growth **198/199**, 511 (1999).

[19] W. Boujelben, M. Ellouze, A. Cheikh-Rouhou, J. Pierre, Q. Cai, W. B. Yelon, K. Shimizu, and C. Duroourdieu, Phys. Status Solidi A **191**, 243 (2002); W. Boujelben, A. Cheikh-Rouhou, M. Ellouze, and J. C. Joubert, *ibid.* **177**, 503 (2000).

[20] N. Rama, J. B. Philipp, M. Opel, A. Erb, V. Sankaranarayanan, R.

Gross, and M. S. R. Rao, Eur. Phys. J. B **38**, 553 (2004).

[21] N. Guiblin, D. Grebille, C. Martin, and M. Hervieu, J. Solid State Chem. **177**, 3310 (2004).

[22] V. Markovich, I. Fita, A. I. Shames, R. Puzniak, E. Rozenberg, C. Martin, A. Wisniewski, Y. Yuzhelevskii, A. Wahl, and G. Gorodetsky, Phys. Rev. B **68**, 094428 (2003).

[23] J.-G. Park, M. S. Kim, H.-C. Ri, K. H. Kim, T. W. Noh, and S.-W. Cheong, Phys. Rev. B **60**, 14 804 (1999).

[24] V. Markovich, G. Jung, Y. Yuzhelevski, G. Gorodetsky, A. Szewczyk, M. Gutowska, D. A. Shulyatev, and Ya. M. Mukovskii, Phys. Rev. B **70**, 064414 (2004); Y. Yuzhelevski, V. Markovich, V. Dikovsky, E. Rozenberg, G. Gorodetsky, G. Jung, D. A. Shulyatev, and Ya. M. Mukovskii, *ibid.* **64**, 224428 (2001); V. Markovich, Y. Yuzhelevskii, G. Gorodetsky, G. Jung, C. J. van der Beek, and Ya. M. Mukovskii, Eur. Phys. J. B **35**, 295 (2003).

[25] G. Jung, V. Markovich, Y. Yuzhelevskii, E. Rozenberg, G. Gorodetsky, and Ya. Mukovskii, J. Appl. Phys. **97** 10H708 (2005).

[26] T. Penney, M. W. Shater, and J. B. Torrance, Phys. Rev. B **5**, 3669 (1972).

[27] C. Cui and T. A. Tyson, Appl. Phys. Lett. **84**, 942 (2004); Phys. Rev. B **70**, 094409 (2004).

[28] V. Markovich, I. Fita, R. Puzniak, A. Wisniewski, and G. Gorodetsky, (unpublished).

[29] I. V. Medvedeva, C. Martin, Yu. S. Bersenev, V. Morshchakov, K. Barner, and B. Raveau, Phys. Met. Metallogr. **97**, 169 (2004).

[30] P. Postorino, A. Congeduti, P. Dore, A. Sacchetti, F. Gorelli, L. Ulivi, A. Kumar, and D. D. Sarma, Phys. Rev. Lett. **91**, 175501 (2003).

[31] P. G. Radaelli, G. Iannone, M. Marezio, H. Y. Hwang, S. W. Cheong, J. D. Jorgensen, and D. N. Argyriou, Phys. Rev. B **56**, 8265 (1997).

[32] P. Postorino, A. Sacchetti, M. Capone, and P. Dore, Phys. Status Solidi B **241**, 3381 (2004).

[33] A. Sacchetti, P. Postorino, and M. Capone, cond-mat/0402279 (2004) (unpublished).

[34] F. Rivadulla, J. Rivas, and J. B. Goodenough, Phys. Rev. B **70**, 172410 (2004).

[35] C. P. Bean and D. S. Rodbell, Phys. Rev. **126**, 104 (1962).

[36] V. P. Dyakonov, I. Fita, E. Zubov, V. Pashchenko, V. Mikhaylov, V. Prokopenko, Yu. Bukhantsev, M. Arciszewska, W. Dobrowolski, A. Nabialek, and H. Szymczak, J. Magn. Magn. Mater. **246**, 40 (2002).

[37] J. A. Mydosh, *Spin Glasses* (Taylor and Francis, London, 1993).

[38] R. Laiho, E. Lahderanta, J. Salminen, K. G. Lisunov, and V. S. Zakhvalinskii, Phys. Rev. B **63**, 094405 (2001).